HER-2-mediated endocytosis of magnetic nanospheres and the implications in cell targeting and particle magnetization

Shy Chyi Wuang[†,‡], **Koon Gee Neoh**[†,*], **En-Tang Kang**[†], **Daniel W. Pack**[‡], and **Deborah E. Leckband**[‡]

† *Department of Chemical and Biomolecular Engineering National University of Singapore Kent Ridge, Singapore 119260*

‡ *Department of Chemical and Biomolecular Engineering University of Illinois, Urbana-Champaign Urbana, IL 61801, USA*

Abstract

Polypyrrole-Fe_3O_4 nanospheres were synthesized via an emulsion polymerization method with hyaluronic acid as the surfactant. Hyaluronic acid offers the advantages of biocompatibility, cell adhesive property and the availability of functional groups for attachment of other molecules. The nanospheres were further functionalized with herceptin, and the efficacy of uptake of the functionalized nanospheres by human breast cancer cells was evaluated. It is envisioned that the combination of hyaluronic acid with its cell adhesive property and herceptin would result in high efficacy of internalization of the nanospheres by the cancer cells via a HER-2-mediated endocytosis. Our results showed that this is indeed the case and that the high concentration of herceptin-functionalized magnetic nanospheres in the cancer cells offers great potential in cancer cell-targeting and treatment. In addition, the magnetic property of these nanospheres was also critically investigated and magnetization was found to be affected by the particles' environment. The combination of these cell-targeting magnetic carriers with chemotherapeutic agents will be highly advantageous for the preferential killing of cancer cells in hyperthermia treatment.

Keywords

Polypyrrole-Fe_3O_4 nanospheres; herceptin; HER-2; mediated endocytosis; cell-targeting; magnetization

1. Introduction

In recent years, magnetic particles have found application in numerous biological fields such as in diagnostics, drug targeting, molecular biology, cell isolation and purification, and as hyperthermia causing agents for cancer therapy [1,2]. Many of these applications require the magnetic particles to possess cell targeting property especially in the case of cancer diagnosis and treatment. Efforts in conferring cell targeting property onto the magnetic nanoparticles include the modification of the particles with chemotherapeutic agents [3,4], ligands [4,5] and antibodies [6]. These agents usually enter the target cells via endocytosis.

*Corresponding author: Professor K.G. Neoh, Department of Chemical and Biomolecular Engineering, National University of Singapore, Kent Ridge, Singapore 119260, Tel:+65-65162176 Fax:+65-67791936 Email: chenkg@nus.edu.sg.

Endocytosis is an important pathway by which drugs and chemotherapeutic agents enter cells. It is also the most studied mechanism for cell targeting and uptake. Cells will endocytose solutes from their extracellular environment through one of following processes [7,8]: (i) fluid-phase endocytosis, where the solute to be endocytosed is present within the extracellular fluid bathing the cell surface and some of the extracellular fluid is captured within the lumen of the budding endocytic vesicle; (ii) adsorptive endocytosis, where the solute that is to be endocytosed binds to the cell surface through non-specific mechanisms; (iii) receptor-mediated endocytosis, where a solute will bind to its cognate cell membrane receptor to elicit either a constitutive or ligand-stimulated internalization.

Recently, efforts in tumor cell biology have resulted in the availability of more specific anticancer chemotherapeutic agents which can exhibit less toxicity on normal cells. Herceptin is a humanized IgG monoclonal antibody directed against the extracellular domain of the human epidermal growth factor receptor 2 (HER-2), which is expressed in some types of breast cancer cells [9,10]. HER-2 has been widely researched on as a therapeutic target in breast cancer because it is widespread in tumors and HER-2 levels correlate strongly with the pathogenesis and prognosis of breast cancer [11]. HER-2 is also an easily accessible cell surface receptor overexpressed on the primary tumour as well as on metastatic sites [12], indicating that anti-HER-2 therapy may be effective in all disease sites. The internalization ability of HER-2 allows an efficient uptake of the herceptin antibody alone as well as when conjugated to drugs or drug carrier systems. Hyaluronic acid (HA) or hyaluronan, a naturally occurring glycosaminoglycan in the extracellular matrix, is synthesized at the cell membranes [13] and readily forms a pericellular matrix in culture. In tumors, small amounts can be seen between cancer cells but it accumulates mainly in the stroma that surrounds epithelial cancer cell clusters [14]. Cancer cells exhibit receptors such as CD44 and RHAMM which interact with HA. High HA levels are associated with many cancers, and it has been demonstrated that inhibition of endogenous hyaluronan synthesis dramatically reduces tumor growth in vivo [15].

Previously, we have reported the preparation of polypyrrole (PPY)-Fe_3O_4 nanospheres stabilized using polyvinyl alcohol [16] or hyaluronic acid [17] and their potential application in cancer cell targeting and treatment. In the current work, we report on the preparation of herceptin-functionalized HA–stabilized magnetic nanospheres and the endocytosis of these nanospheres by human breast cancer cells, with emphasis on the behavioural magnetization of the nanospheres. The functionalization of the nanospheres with herceptin utilized the COOH groups of the latter instead of the amine groups as reported in our earlier communication [17]. We found that the presence of herceptin on the surface of the nanospheres greatly enhanced their uptake via endocytosis by SK-Br-3 cells. Using suitable controls, these observations are attributed mainly to a HER-2-mediated endocytosis. In contrast to the non-functionalized nanospheres, these herceptin-functionalized nanospheres were able to elicit a cytotoxic effect in vitro. In addition, it was found that the magnetization profiles of the nanospheres vary with the surrounding environment, illustrating the importance of in-vitro conditions of magnetization measurement to accurately reflect the in-vivo capability of the magnetic nanospheres. In view of the efficient cancer cell-targeting properties, cytotoxic effects and favourable magnetization values, these nanospheres may be utilized in cancer therapy, particularly in hyperthermia since the magnetization of these nanospheres correlates directly to their effectiveness as hyperthermia seeds.

2. Experimental

2.1 Methods and Materials

HA potassium salt from human umbilical cord, sodium dodecyl sulfate, pyrrole, oleic acid (90%), N-boc ethylenediamine and McCoy's 5A media were purchased from Sigma-Aldrich Co. Iron (III) chloride, iron (II) chloride tetrahydrate and ammonia solution (25%) were from

Merck Co. Herceptin was obtained as a gift from Genentech Inc. Human breast cancer cells (SK-Br-3) were from ATCC. The other solvents and reagents were of analytical grade and used without further purification.

2.2 Synthesis of Fe_3O_4 nanoparticles and PPY-Fe_3O_4 nanospheres

The syntheses of Fe_3O_4 nanoparticles (MNP) and PPY-Fe_3O_4 nanospheres have been reported previously [17], and slight modifications were done to the latter procedure in this work. The magnetite ferrofluid (0.5 g magnetite in 2.5 ml hexane) was added to 5ml of distilled (DI) water containing 0.2 g of sodium dodecyl sulfate (SDS) which coats the MNP to form an aqueous dispersion of MNP. The mixture was stirred for 1 h before hexane was evaporated at 80°C. Pyrrole was then added, and the mixture was stirred for 1 h to form the magnetite-monomer dispersion. This dispersion was added dropwise to the oxidant ($FeCl_3$) solution containing 5 mg/ml of HA in DI water in an ice-cooled sonication bath. The oxidant:monomer molar ratio was kept at 0.5. The reaction mixture was transferred from the sonication bath to a stirring plate after 3 h. Polymerization was allowed to take place for a further 20 h at room temperature. The nanospheres were washed several times with hexane until no free magnetite could be detected in the rinse, and then washed thrice with DI water. The resulting PPY-Fe_3O_4 nanospheres, denoted by NS, were then dried using a lyophilizer.

2.3 Functionalization of NS with herceptin

The NS were first reacted with N-boc ethylenediamine to introduce amine groups onto the NS to form NS-(NH_2). Fifty mg of 1-ethyl-3-(3-dimethylamino)-propyl carbodiimide (EDC), 20 mg of N-hydroxysuccinimde (NHS) and 2 mg of N-boc ethylenediamine were added to 20 mg of NS in 3 ml of DI water. Triethylamine was used to adjust the pH of the reaction mixture to 8. After 4 h of reaction at room temperature, the nanospheres were washed several times with DI water and dried under reduced pressure. After drying, the nanospheres were stirred with 50% trifluoroacetic acid in dichloromethane for 1 h at room temperature to remove the boc groups. Herceptin was then attached to the surface of NS using carbodiimide chemistry. The nanospheres were dispersed in 3 ml of 0.1 M PBS and placed in an ultrasonic bath for 30 min. 20 mg of NHS and 0.1 g of EDC were then added followed by 0.5 ml of herceptin (20 mg/ml in bacteriostatic water for injection). The pH of the reaction mixture was adjusted to 8 using triethylamine. The reaction was allowed to take place for 4 h at room temperature. The resulting particles (denoted by NS-HER) were collected by centrifugation at 5000 rpm, washed several times with DI water and dried under reduced pressure. The amount of herceptin bound to NS was quantified using the Easy-Titer Human IgG (H ± L) assay kit (Pierce). After washing, a sample of NS-HER in DI water was appropriately diluted and used in the assay. The absorbance at 405 nm was measured with SpectraMax 340_{PC} microplate spectrophotometer (Molecular Devices) and herceptin concentration was calculated from a previously determined calibration using standard solutions of herceptin.

2.4 Characterization of as-synthesized and functionalized PPY-Fe_3O_4 nanospheres

Electron microscopy and dynamic light scattering—Transmission electron microscopy (TEM) images of the nanospheres were obtained using a Philips CM12 TEM instrument at an accelerating voltage of 120 kV. Very dilute concentrations of the nanospheres were prepared for observation under the TEM in order to obtain clear images of the individual nanospheres. Particle size was obtained from dynamic light scattering measurements of the nanospheres' dispersion in DI water performed on the 90Plus Particle Size Analyzer (Brookhaven Instruments) at room temperature (25°C). Triplicate samples were used and for each sample, five measurements were collected.

Surface properties—X-ray photoelectron spectrometry (XPS) analysis of the as-synthesized and herceptin-functionalized NS (NS and NS-HER respectively) was made on Kratos Axis ULTRA X-ray photoelectron spectrometer using the monochromatized Al Kα X-ray source (1486.6 eV photons) at a constant dwell time of 100 ms and a pass energy of 40 eV. The anode voltage was 10 kV and the anode current was 10 mA. The pressure in the analysis chamber was maintained at 3×10^{-7} Pa or lower during measurement. The core-level signals were obtained at a photoelectron take-off angle of 90° (with respect to the sample surface). To compensate for surface charging effect, all core-level spectra were referenced to the C 1s hydrocarbon peak at 284.6 eV. In spectral deconvolution, the linewidth (full width at half-maximum) of the Gaussian peaks was maintained constant for all components in a particular spectrum. Zeta-potentials of the nanospheres in DI water were measured using a 90Plus Zeta Potential Analyzer (Brookhaven Instruments) at room temperature. Triplicate samples were used and for each sample, five measurements were collected.

Iron content determination—The iron content of the nanospheres was determined by dissolving a weighed amount of the sample with 70% nitric acid at 40ºC for 30 min and diluting the solution for iron quantification using inductively coupled plasma (ICP) mass spectrometry (Perkin Elmer- Sciex Elan Drce ICP-MS).

2.5 Uptake of nanospheres by cancer cells and cytotoxicity assays

Human breast cancer cells (SK-Br-3) were routinely cultured at 37°C in a humidified atmosphere with 5% CO_2 (in air), in 60 mm Petri dishes containing McCoy's 5A medium, supplemented with 10% fetal bovine serum (FBS), 2 mM L-glutamine and 100 U/ml penicillin-streptomycin. For subculture, the cells were washed once with phosphate-buffered saline (PBS) and incubated with trypsin-EDTA solution (0.25% trypsin, 1mM EDTA) for 5–10 min at 37° C to detach the cells. Complete medium were then added in the flask at room temperature to inhibit the effect of trypsin. The cells were collected by centrifugation and resuspended in the complete medium for reseeding and growth in new culture flasks. Cell viability was determined through staining with Trypan Blue and cells were counted using a hemocytometer. Cell density was estimated using a 0.9 mm^3 counting chamber.

To study the cellular uptake of nanospheres via optical microscopy, the nanospheres were added to the cell culture medium at a concentration of 0.2 mg/ml. The cells were first seeded in 24-well polystyrene dishes for 20 h, after which the medium was replaced with the nanospheres-dispersed culture medium. The nanospheres were sterilized with UV irradiation for 30 min before use. After various periods of incubation at 37°C and 5% CO_2, the cells were washed with PBS and viewed under a Nikon Eclipse TS100 microscope. For quantification of the intracellular uptake of the nanospheres, cells were grown in 6-well culture plates, with approximately 5×10^5 cells in 2 ml of medium. After incubation at 37°C for 20 h, the medium was replaced with one containing the nanospheres at a concentration of 0.2 mg/ml. In control cultures, the cells were seeded at the same cell density and grown in 2 ml of medium without the nanospheres. To investigate the competitive effects of free herceptin on the endocytosis of NS-HER, the seeded cells were first treated with medium containing 200 μg/ml of herceptin for 30 min. After 30 min, the medium was replaced by one containing 0.2 mg/ml of NS-HER and 200 μg/ml of herceptin. The cells were collected after 2, 4 and 24 h of incubation and the intracellular iron concentration quantified. The cells were first washed several times with PBS, detached, resuspended, counted, centrifuged down, and the cell pellet was then dissolved in 70% nitric acid at 40°C for 30 min. The samples were diluted to an estimated final iron concentration of 0.03 – 0.3 μg/ml for ICP analysis. The Fe concentration of the sample was calculated from the calibration curve obtained using standard Fe solutions of various concentrations. Three sets of duplicates were measured done for each condition and the results were averaged.

For TEM viewing, the cell pellet was fixed in a Karnovsky's fixative in phosphate buffered saline with 2% glutaraldeyde and 2.5% paraformaldehyde. Microwave fixation was used with this primary fixative and the cell pellet was then washed in cacodylate buffer with no further additives. Microwave fixation was also used with the secondary 2% osmium tetroxide fixative, followed by the addition of 3% potassium ferricyanide for 30 min. After washing with water, saturated uranyl acetate was added for Enbloc staining. The cells were then dehydrated in a series of increasing concentrations of ethanol. Acetonitrile was used as the transition fluid between ethanol and the epoxy. Infiltration series was done with an epoxy mixture using the Epon substitute L × 112. The resulting blocks were polymerized at 90°C overnight, trimmed and ultra-thinly sectioned with diamond knives. Sections were stained with uranyl acetate and lead citrate, and examined or photographed with a Hitachi H600 Transmission Electron Microscope.

The cytotoxicity of NS-HER and NS was evaluated by determining the viability of SK-Br-3 cells after incubation with the medium containing the nanospheres. The cytotoxic effects of the combinations of NS and herceptin (at herceptin concentrations ranging from 20 ng/ml to 100 μg/ml) were also studied. Cell viability testing was carried out via the reduction of the MTT reagent (3-[4,5-dimethyl-thiazol-2-yl]-2,5-diphenyltetrazolium bromide, Sigma). The MTT assay was performed in a 96-well plate following the standard procedure with minor modifications. The nanoparticles were sterilized with UV irradiation for 30 min before use. Control experiments were carried out using the complete growth culture medium only (non-toxic control), and with 1% Triton X-100 (Sigma) (toxic control). Cells were first seeded at a density of 5×10^3 cells/well for 20 h before the medium was replaced with one containing the nanoparticles at 0.2 mg/ml. The cells were incubated at 37°C and 5% CO_2 for 2, 24, 48 and 72 h. The culture medium from each well was then removed and 90 μl of medium and 10 μl MTT solution (5 mg/ml in PBS) were then added to each well. After 4 h of incubation at 37 ° C and 5% CO_2, the medium was removed and the formazan crystals were solubilized with 100 μl dimethyl sulphoxide (DMSO) for 15 min. The optical absorbance was then measured at 570 nm on a SpectraMax 340_{PC} microplate spectrophotometer (Molecular Devices). The results were expressed as percentages relative to the results obtained with the non-toxic control. The differences in the results obtained with the various samples and the controls were analyzed statistically using the two sample t-test. The differences observed between samples were considered significant for $P < 0.05$.

2.6 In vitro magnetization studies

The magnetization measurements were performed at room temperature using a Superconducting Quantum Interference Device (SQUID) (MPMS, Quantum design), with a saturating field of 1T. The nanospheres were tested under three different conditions: (a) solid particles, (b) particles dispersed in cell culture medium with 1% agarose, and (c) endocytosed particles within cells dispersed in cell culture medium with 1% agarose, at room temperature. The magnetization values were normalized to the mass of Fe in the nanospheres to yield the specific magnetization, M_s (emu/g Fe).

3. Results and Discussion

3.1 Preparation of NS-HER

The schematic for the preparation of NS-HER is given in Figure 1. The carboxyl groups of the surface HA were first reacted with N-boc ethylenediamine. After the boc group was removed by treatment with trifluoroacetic acid, herceptin was then attached to the amine groups on NS (NH_2). The success of the functionalization of herceptin was ascertained by XPS. The C 1s core-level spectra of NS(NH_2) and NS-HER and herceptin were compared in Figure 2. The C 1s core-level spectrum of NS(NH_2) (Figure 2a) consists of five peak components with binding

energies at about 284.6, 285.8, 286.2, 288 and 288.6eV, which can be fitted to C-C/C-H, C-N, C-O, N-C=O and O-C=O respectively [18,19]. The C-N, C-O, N-C=O and O-C=O species are due primarily to the surface HA, the introduced amine groups as well as the amide linkages formed between these two species. After herceptin immobilization, the C 1s core-level spectrum of NS-HER (Figure 2b) shows significantly enhanced C-N, C-O and N-C=O peaks relative to the C-C/C-H peak. These are consistent with those in herceptin (Figure 2c) and the formation of new amide linkages formed during the functionalization (which contributes to the N-C=O species). The amount of herceptin bound to NS was determined to be about 1.4 mg/g nanospheres using the Easy-Titer Human IgG (H + L) assay kit.

Table 1 summarizes and compares the properties of NS and NS-HER. The % Fe in these two types of nanospheres remained similar, which is expected since the amount of immobilized herceptin did not increase the non-magnetic component of the nanospheres significantly. The zeta-potential, however, became less negative upon herceptin functionalization, likely due to the reduction in $-COO^-$ groups which were used for the attachment of N-boc ethylenediamine for subsequent attachment of herceptin. The morphology of both NS and NS-HER is similar under the TEM, though more clumping was observed for NS-HER. This observation is reflected in their hydrodynamic diameters (D_H), where NS-HER has a much larger D_H (~750 nm as compared to the ~420 nm of NS) which can be attributed to some degree of cross-linking between the amino and carboxyl groups of herceptin on different nanospheres. The D_H of NS (~420 nm) was much higher than what we have previously reported (~210 nm)[17]. The differences could be due to the use of different methods of dispersion during the initial period of polymerization (bath sonication in the current protocol as opposed to high speed stirring in the previous method) and/or the different HA salt. The size of the individual nanosphere, however, remained at about 100 nm in diameter, as can be seen from Table 1. Despite the relative larger effective size of NS-HER, they are effectively taken up by cancer cells as will be discussed in the next section.

3.2 Endocytosis of NS-HER by SK-Br-3

Throughout the duration of this experiment, no significant differences in cell morphology were observed when compared to the control SK-Br-3 cells cultured with no nanospheres. The cells appeared either circular or spread out. As observed under an optical microscope, the amount of nanospheres associated with the cells was the greatest in the case of NS-HER, whereas there was little association of the nanospheres with the cells incubated with NS or with NS-HER pre- and co-treated with 200 μg/ml of free herceptin. These observations were supported by the quantification of the amount of iron associated with the cells, as shown in Figure 3. The iron association observed with NS (4.6 ± 0.7, 5.1 ± 0.7 and 9.1 ± 3.1 pg/cell at 2, 4 and 24 h respectively) may be facilitated by the adhesive properties of the nanospheres imparted by the surface HA, since HA has been implicated in cancer cell adhesion and as a central component of the distinct stroma that surrounds and probably supports tumors [20]. The iron association of the NS-HER by SK-Br-3 cells was 21.9 ± 4.7 pg/cell at 2 h, 27 ± 4.2 pg/cell at 4 h and increased to 69.6 ± 4.6 pg/cell at 24 h which are several times greater than those of NS. These observations are in agreement with our previous work which showed a 7-fold increase in the internalization of herceptin-functionalized particles over the non-functionalized ones by HCC1954 cells [17]. Other reports have also showed that incorporation of liposomes into HER-2-overexpressing cancer cells (such as SK-Br-3) was herceptin-dependent [21] and herceptin-conjugated moieties can be used for cancer-targeting probes [6,22,23]. When the SK-Br-3 cells were treated with free herceptin to investigate any effect of competitive inhibition, the uptakes of NS-HER were reduced greatly to 5.8 ± 1.6 pg/cell at 2 h and remained low at 6.7 ± 1.8 pg/cell at 24 h. These levels are comparable with those for NS (Figure 3), and indicate that the free herceptin in the medium binds to the HER-2 receptors on the SK-Br-3 cells and effectively prevents NS-HER from interacting with these receptors. To confirm that

the nanospheres are endocytosed by the cells and not just superficially associated with the cells, TEM studies were done on the cells after 4 h incubation with medium containing NS-HER or NS-HER with free herceptin. The TEM images clearly show the endocytosed NS-HER inside the cells (Figure 4a) while for the cells that were pre- and co-treated with herceptin (Figure 4b), no nanospheres were observed inside the cells. With cells incubated with NS (result not shown), there was also little or no intracellular nanospheres. The endocytosis of NS-HER was also largely blocked after a 4 h incubation at 4ºC, with iron content at <20% of that observed at 37ºC, similar to that for cells incubated with NS-HER together with free herceptin. This is in line with the observations made by others [24,25] that internalization does not occur at 4ºC. For comparison purposes, control experiments with NS and NS-HER at 37°C were carried out with a low HER-2 expressing breast cancer cell line, MDA-MB-231. The results showed that the differences between the iron associations of NS and NS-HER were small. Table 2 summarizes the iron association data for the 2 cancer cell lines (SK-Br-3 and MDA-MB-231). These observations confirm that herceptin-mediated endocytosis is the predominant mechanism for the uptake of NS-HER.

The increasing uptake of NS-HER with time and the differences between the uptakes of NS and NS-HER by SK-Br-3 cells are likely due to a rapid association of NS-HER with the HER-2 receptors, coupled with a slow internalization rate of the HER-2 receptors. Hendriks and coworkers [26,27] reported a high HER-2 recycling fraction of 0.94 and a low internalization rate constant of ~0.01 min^{-1}. This slow internalization rate of the HER-2 receptors coupled with the high levels of free herceptin present in the cell medium in the herceptin pre- and co-treatment experiments also explained the prevalence of competitive inhibition throughout the duration of the experiments.

Following the verification of the cell-targeting properties of NS-HER via a HER-2-mediated endocytosis, we investigated the activity of the immobilized herceptin on NS-HER by measuring the viabilities of cells incubated with NS-HER and NS with various concentrations of free herceptin. Herceptin treatment of SK-Br-3 cells frequently results in reduced cell replication [28,29] since herceptin is known to have an anti-proliferative effect to HER-2 expressing cells [30]. Such effects can be reflected in cytotoxicity assays. As shown in Figure 5, the viability of the cells incubated with NS-HER fell to about $55 \pm 2\%$ after 2 h and $48 \pm 2\%$ at 24 h, and it continued to decrease, reaching a value of $30 \pm 12\%$ after 72 h. With NS, the cell viability remained high initially and decreased gradually to about 85% after 72 hr. It has been shown in Figure 3 that the uptake of NS-HER by the cells is significantly higher than that of NS. The higher cytotoxicity of NS-HER may thus be due to herceptin and/or the nanospheres. To investigate how herceptin may have contributed to the observed cytotoxicity of NS-HER, the cells were incubated with NS and free herceptin ranging from 20 ng/ml to 100 μg/ml. No immediate cytotoxicity was observed but the viabilities decreased gradually with time. Increasing the herceptin concentration from 20 ng/ml to 100 μg/ml did not result in any further reduction in cell viability. Saturation of HER-2 receptors may be responsible for this observation. It should be noted that control experiments using only 10 and 100 μg/ml of free herceptin without any nanospheres gave very similar results to those obtained with co-incubation of NS and free herceptin. Thus, it appears that herceptin has contributed to the cytotocity of the cells, but is probably not the only contributing factor. Herceptin has been reported to show no direct anti-proliferative or growth inhibition effects against cancer cells in vitro regardless of HER-2 expression [31,32], and Mandler and co-workers found that higher concentrations of herceptin did not have significant effects on in-vitro viabilities [33]. In contrast, other reports have shown a dose-dependent growth reduction with herceptin [34,35]. While seemingly contradicting, these results suggest that the anti-tumor effect of herceptin involves more than one direct mechanism [36,37].

Since it was unlikely that the cytotoxicity observed with NS-HER was due solely to the immobilized herceptin (the amount of immobilized herceptin in the media is ~ 280 ng/ml) from the above observations, we investigated other possibilities such as the deleterious effects of the endocytosed NS-HER on the cells including that caused by the SDS-coated Fe_3O_4. We have also performed the cytotoxicity assay using other cell lines (MCF-7, MDA-MB-231 and RAW264.7) and found that the cytotoxicity effects of NS-HER on the tested cancer cells are related to the extent of uptake by these cells (results not shown). With the macrophagic RAW264.7 cells, an initial decrease in viability was observed but the viabilities gradually recovered to 100% with time despite an increasing iron association, possibly due to their innate versatility as phagocytes. Thus, the other cause of cytotoxicity of NS-HER on SK-Br-3 cells may be the combined effects of the SDS-coated Fe_3O_4 and the PPY. When the MTT assay was done with 0.1 mg/ml of SDS, the cells showed immediate cytotoxicity, with a viability at ~72% after 2 h and this decreased to 2 % after 24 h. On lowering the SDS concentration to 0.05 mg/ml, cytotoxicity was not observed, with viability remaining high even after 24 h. After endocytosis of NS-HER into the cells, the intracellular SDS concentration may reach much higher values as compared to that of the extracellular medium, and affect the cells' viability. On the other hand, incubation of herceptin-functionalized PPY nanospheres (without encapsulated Fe_3O_4) with the cells resulted in no immediate cytotoxicity with viability at 96 % at 2 h but cytotoxic effects set in at 24 h, with viability of the cells measured to be 59 %. In lieu of these results, the much higher cytotoxicity observed with NS-HER as compared to NS can be attributed both to the bound herceptin as well as the higher uptake of NS-HER by the cells with the consequence of a much higher intracellular concentration of PPY as well as SDS-coated Fe_3O_4.

With the excellent cell-targeting capability and uptake-related cytotoxicity, NS-HER can potentially be of enormous use in cancer therapy. For example, Ito and co workers [21] reported that an amount of 15.6 ± 0.27 pg magnetite/cell (~11 pg Fe/cell) was sufficient for use in hyperthermia. The iron association achieved in our study is much greater than this and therefore the nanospheres can be expected to be highly desirable as hyperthermia agents. Besides, many chemotherapeutics including paclitaxel [38], pertuzumab [29], carboplatin, doxorubin and epirubicin [28] have additive or synergistic effects with herceptin and a combination of NS-HER with these chemotherapeutics may prove advantageous in cancer therapy.

3.3 In vitro magnetization studies

The M_s curves of NS-HER in different environments are illustrated in Figure 6. The M_s of solid NS-HER is 75 emu/g Fe, and this decreases to 42 emu/g Fe in a gel-like medium (cell medium with 1% agarose). The M_s value of the Fe_3O_4 particles used in its synthesis is 91 emu/g Fe, which is lower than what we have previously reported [16,39], possibly due to a different method of M_s determination (VSM in the earlier work and SQUID in the current work). While we did not see a significant decrease in M_s (expressed in terms of emu/g Fe) between Fe_3O_4 and the PPY- Fe_3O_4 nanospheres when using PVA as the surfactant [16], we observed a decrease in this work when HA was used as the surfactant (91 emu/g Fe for Fe_3O_4 and 75 emu/g Fe for NS). Magnetic properties can be altered by the sorption of surfactants [40] and the stabilization of magnetite particles by surfactants has been shown to decrease the value of saturation magnetization [41], which can result from a pinning of the surface spins and a related increase in the magnetic anisotropy energy constant [42]. The surfactants (PVA and HA) probably change the interparticle interactions differently which in turn affect the magnetization of the system [43].

As shown in Figure 6a, solid NS-HER gives a sigmoidal shaped M_s curve which is typical of superparamagnetic substances. When NS-HER are dispersed in cell medium with 1% agarose, the M_s curve changed to one with negative sloping ends after the peak magnetization is reached.

The diamagnetism of the surrounding cell medium has superposed a negative slope at higher magnetic fields (>2000 Oe), a phenomenon that has been reported by several others [41,44]. After being endocytosed by the SK-Br-3 cells following a 4 h incubation, the M_s curve of the endocytosed NS-HER (Figure 6c) deviates more significantly from the regular sigmoid. It exhibits a negative slope at a smaller magnetic field of about 600 Oe. Using the peak magnetization at magnetic field of 500 Oe, a conservative specific magnetization of these endocytosed NS-HER was calculated to be 24 emu/g Fe, much lower than the NS-HER in the previous two conditions (i.e. as dry solid and suspended in cell medium). This could be due to additional diamagnetic contribution from the cells and a possible shielding effect of the nanospheres from the extracellular environment. The mediocre match between the magnetization and demagnetization curves also seems to suggest some form of interaction between the cells and the endocytosed nanospheres. While these results do not confirm the presence of any cell-particle interactions, they indicate that the surrounding environment has to be taken into account when using magnetization data since the apparent magnetization may be much lower in a gel-like medium (which is more similar to the tissue environment) than in the solid state (where magnetization values are frequently reported). In addition, a lower external magnetic field can elicit the maximum magnetization of the nanospheres in the earlier case.

4. Conclusion

HA–stabilized magnetic nanospheres have been prepared and functionalized with the cancer antibody herceptin. These nanospheres were endocytosed by cancer cells to a large extent via a receptor-mediated mechanism where the functionalized herceptin on the nanospheres targets the HER-2 receptors on the cancer cells. The uptake of these nanospheres reached > 7 times that of the non-functionalized ones. While our initial aim was to investigate how the anti-tumor effects of herceptin can be combined with magnetic nanospheres for use in hyperthermia, we incidentally found an uptake-associated cytotoxic effect on the cancer cells. This can potentially be exploited in cancer treatment as only cells expressing the HER-2 receptors endocytose large amounts of the herceptin-functionalized nanospheres. Moreover, these nanospheres have the magnetic properties to be considered as promising hyperthermia agents. On the other hand, the measured magnetization of the nanospheres was lower in a more fluid medium as compared to in the solid state, and the diamagnetic nature of the tissue environment may result in a diminished apparent magnetization. This important effect of the particles' environment on their magnetization profiles should be taken into consideration when comparing magnetization values.

References

1. Pankhurst QA, Connolly J, Jones SK, Dobson J. Applications of magnetic nanoparticles in biomedicine. J Phys D: Appl Phys 2003;36:R167–181.
2. Safarik, I.; Safarikova, M. Overview of magnetic separations used for biochemical and biotechnological applications. In: Hafeli, U.; Schutt, W.; Teller, J.; Zborowski, M., editors. Scientific and clinical applications of magnetic carriers. New York: Plenum Press; 1997. p. p323-340.

3. Alexiou C, Arnold W, Klein RJ, Parak FG, Hulin P, Bergemann C, et al. Locoregional cancer treatment with magnetic drug targeting. Cancer Res 2000;60:6641–6648. [PubMed: 11118047]

4. Alexiou C, Schmid RJ, Jurgons R, Kremer M, Wanner G, Bergemann C, et al. Targeting cancer cells: magnetic nanoparticles as drug carriers. Eur Biophys J 2006;35:446–450. [PubMed: 16447039]

5. Mäntylä T, Hakumäki JM, Huhtala T, Närvänen A, Ylä-Herttuala S. Targeted magnetic resonance imaging of scavidin-receptor in human umbilical vein endothelial cells in vitro. Magn Resonance Med 2006;55:800–804.

6. Huh YM, Jun YW, Song HT, Kim S, Choi J-S, Lee J-H, et al. In vivo magnetic resonance detection of cancer by using multifunctional magnetic nanocrystals. J Am Chem Soc 2005;127:12387–12391. [PubMed: 16131220]

7. Smith MW, Gumbleton M. Endocytosis at the blood–brain barrier: From basic understanding to drug delivery strategies. J Drug Targeting 2006;14:191–214.

8. Mukherjee S, Ghosh RN, Maxdield FR. Endocytosis. Physiol Rev 1997;77:759–803. [PubMed: 9234965]

9. Steinhauser I, Spänkuch B, Strebhardt K, Langer K. Trastuzumab-modified nanoparticles: Optimisation of preparation and uptake in cancer cells. Biomaterials 2006;27:4975–4983. [PubMed: 16757022]

10. Moore S, Cobleig MA. Targeting metastatic and advanced breast cancer. Seminars in Oncology Nursing 2007;23:37–45. [PubMed: 17303515]

11. Slamon DJ, Clark GM, Wong SG, Levin WJ, Ullrich A, McGuire WL. Human breast cancer: correlation of relapse and survival with amplification of the HER-2/neu oncogene. Science 1987;235:177–182. [PubMed: 3798106]

12. Nahta R, Esteva FJ. HER-2-targeted therapy: lessons learned and future directions. Clin Cancer Res 2003;9:5078–5084. [PubMed: 14613984]

13. Prehm P. Synthesis of hyaluronate in differentiated teratocarcinoma cells. Biochem J 1983;211:191–198. [PubMed: 6870820]

14. Delpech B, Girard N, Bertrand P, Courel MN, Chauzy C, Delpech A. Hyaluronan: fundamental principles and applications in cancer. J Internal Med 1997;242:41–48. [PubMed: 9260565]

15. Toole BP, Hascall VC. Hyaluronan and tumor growth. American J Pathology 2002;161:745–747.

16. Wuang SC, Neoh KG, Kang ET, Pack DW, Leckband DE. Synthesis and functionalization of polypyrrole-Fe_3O_4 nanoparticles for applications in biomedicine. J Mater Chem 2007;17:3354–3362.

17. Wuang SC, Neoh KG, Kang ET, Pack DW, Leckband DE. Polypyrrole nanospheres with magnetic and cell-targeting capabilities. Macromol Rapid Comm 2007;28:816–821.

18. Moulder, JF.; Stickle, WF.; Sobol, PE.; Bomben, KD. Handbook of X-ray Photoelectron Spectroscopy. Chastain, J., editor. Ch II. Perkin-Elmer; Eden Prairie, Minn: 1992.

19. Beamson, B.; Briggs, D. High Resolution XPS of Organic Polymers: The Scienta ESCA Database. John Wiley-Chichester; 1992.

20. Toole BP, Wight TN, Tammi MI. Hyaluronan-cell interactions in cancer and vascular disease. J Biol Chem 2002;277:4593–4596. [PubMed: 11717318]

21. Ito A, Kuga Y, Honda H, Kikkawa H, Horiuchi A, Watanabe Y, et al. Magnetite nanoparticle-loaded anti-HER2 immunoliposomes for combination of antibody therapy with hyperthermia. Cancer Letters 2004;212:167–175. [PubMed: 15279897]

22. Park JW, Hong K, Carter P, Asgari H, Guo LY, Keller GA, et al. Development of anti-p185[HER2] immunoliposomes for cancer therapy. Proc Natl Acad Sci USA 1995;92:1327–1331. [PubMed: 7877976]

23. Artemov D, Mori N, Okollie B, Bhujwalla AM. MR molecular imaging of the Her-2/neu receptor in breast cancer cells using targeted iron oxide nanoparticles. Magn Reson Med 2003;49:403–408. [PubMed: 12594741]

24. Tsujimoto M, Yip YK, Vilcek J. Tumor necrosis factor: specific binding and internalization in sensitive and resistant cells. Proc Natl Acad Sci USA 1985;82:7626–7630. [PubMed: 2999773]

25. Bradley JR, Johnson DR, Pober JS. Four different classes of inhibitors of receptor-mediated endocytosis decrease tumor necrosis factor-induced gene expression in human endothelial cells. J Immunology 1993;150:5544–5555. [PubMed: 8390537]

26. Hendriks BS, Opresko LK, Wiley HS, Lauffenburger D. Coregulation of epidermal growth factor receptor/human epidermal growth factor receptor 2 (HER2) levels and locations. Cancer Research 2003;63:1130–1137. [PubMed: 12615732]

27. Hendriks BS, Opresko LK, Wiley HS, Lauffenburger D. Quantitative analysis of HER2-mediated effects on HER2 and epidermal growth factor receptor endocytosis. J Biological Chemistry 2003;278:23343–23351.

28. Pegram MD, Konecny GE, O'Callaghan C, Beryt M, Pietras R, Slamon DJ. Rational combinations of trastuzumab with chemotherapeutic drugs used in the treatment of breast cancer. J Natl Cancer Inst 2004;96:739–749. [PubMed: 15150302]

29. Brockhoff G, Heckel B, Schimidt-Bruecken E, Plander M, Hofstaedter F, Vollmann A, et al. Differential impact of Cetuximab, Pertuzumab and Trastuzumab on BT474 and SK-BR-3 breast cancer cell proliferation. Cell Prolif 2007;40:488–507. [PubMed: 17635517]

30. Nahta R, Esteva FJ. Herceptin: mechanisms of action and resistance. Cancer Letters 2006;232:123–138. [PubMed: 16458110]

31. Kimura K, Sawada T, Komatsu M, Inoue M, Muguruma K, Nishihara T, et al. Antitumor effect of trastuzumab for pancreatic cancer with high HER-2 expression and enhancement of effect by combined therapy with gemcitabine. Clin Cancer Res 2006;12:4925–4932. [PubMed: 16914581]

32. Gong SJ, Jin CJ, Rha SY, Chung HC. Growth inhibitory effects of trastuzumab and chemotherapeutic drugs in gastric cancer cell lines. Cancer Letters 2004;214:215–224. [PubMed: 15363548]

33. Mandler R, Kobayashi H, Hinson ER, Brechbiel MW, Waldmann TA. Herceptin-geldanamycin immunoconjugates: Pharmacokinetics, biodistribution, and enhanced antitumor activity. Cancer Res 2004;64:1460–1467. [PubMed: 14973048]

34. Kauraniemi P, Hautaniemi S, Autio R, Astola J, Monni O, Elkahloun A, et al. Effects of herceptin treatment on global gene expression patterns in *HER2*-amplified and nonamplified breast cancer cell lines. Oncogene 2004;23:1010–1013. [PubMed: 14647448]

35. Guan H, Jia SF, Zhou Z, Stewart J, Kleinerman ES. Herceptin down-regulates HER-2/*neu* and vascular endothelial growth factor expression and enhances taxol-induced cytotoxicity of human ewing's sarcoma cells in vitro and in vivo. Clin Cancer Res 2005;11:2008–2017. [PubMed: 15756027]

36. Fendly BM, Winget M, Hudziak RM, Lipari MT, Napier MA, Ullrich A. Characterization of murine monoclonal antibodies reactive to either the human epidermal growth factor receptor or HER2/*neu* gene product. Cancer Res 1990;50:1550–1558. [PubMed: 1689212]

37. Sarup JC, Johnson RM, King KL, Fendly BM, Lipari MT, Napier MA, et al. Characterization of an anti-p185^{HER2} monoclonal antibody that stimulates receptor function and inhibits tumor cell growth. Growth Regul 1991;1:72–82. [PubMed: 1688187]

38. Merlin JL, Barberi-Heyob M, Bachmann N. In vitro comparative evaluation of trastuzumab (Herceptin®) combined with paclitaxel (Taxol®) or docetaxel (Taxotere®) in HER2-expressing human breast cancer cell lines. Annals of Oncology 2002;13:1743–1748. [PubMed: 12419746]

39. Hu FX, Neoh KG, Cen L, Kang ET. Cellular response to magnetic nanoparticles "PEGylated" via surface-initiated atom transfer radical polymerization. Biomacromolecules 2006;7:809–816. [PubMed: 16529418]

40. Morup S. Mössbauer spectroscopy studies of suspensions of Fe_3O_4 microcrystals. J Magn Magn Mater 1983;39:45–47.

41. Dresco PA, Zaitsev VS, Gambino RJ, Chu B. Preparation and properties of magnetite and polymer magnetite nanoparticles. Langmuir 1999;15:1945–1951.

42. Berkowitz AE, Lahut JA, VanBuren CE. Properties of magnetic fluid particles. IEEE Trans Magn 1980;16:184–190.

43. Sorge KD, Thompson JR, Schulthess TC, Modine FA, Haynes TE, Honda S, et al. Oriented, single domain Fe nanoparticle layers in single crystalyttria stabilized zirconia. IEEE Trans Magn 2001;37:2197–2199.

44. Black, RC.; Wellstood, FC. The SQUID Handbook. Clarke, J.; Braginski, AI., editors. II. Wiley-VCH; 2006. p. 396
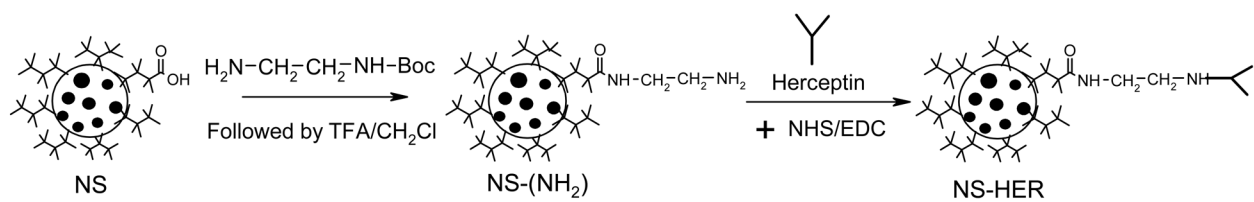
NS: PPY-Fe$_3$O$_4$ nanospheres
NS-(NH$_2$): PPY-Fe$_3$O$_4$ nanospheres linked with N-boc ethylenediamine
NS-HER: Herceptin-functionalized PPY-Fe$_3$O$_4$ nanospheres

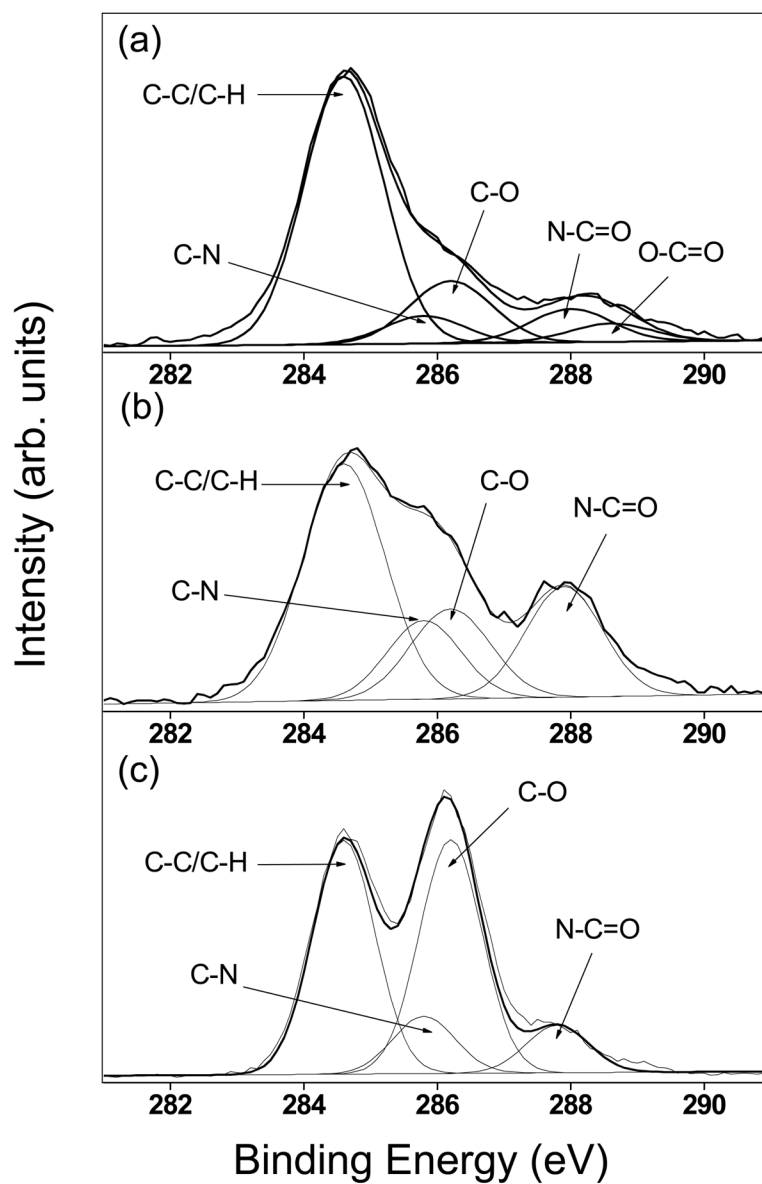**Figure 1.**
Schematic representation of the preparation of NS-HER.

Figure 2.
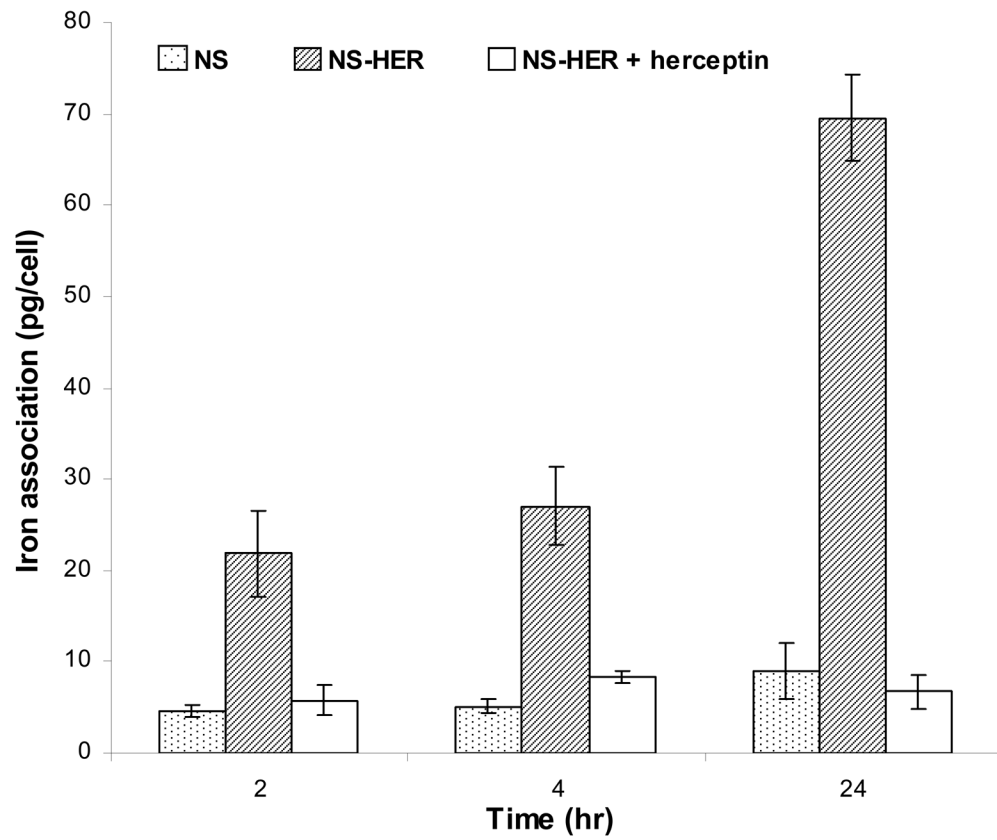XPS C 1s core-level spectra of (a) NS-(NH$_2$), (b) NS-HER and (c) herceptin.

Figure 3.
Amount of iron associated with SK-Br-3 cells after 2, 4 and 24 h incubation with NS, NS-HER and NS-HER with free herceptin. Three sets of duplicates were done for each data point. The iron association of NS-HER is significantly higher ($P < 0.01$) than those for NS and NS-HER at all time points.
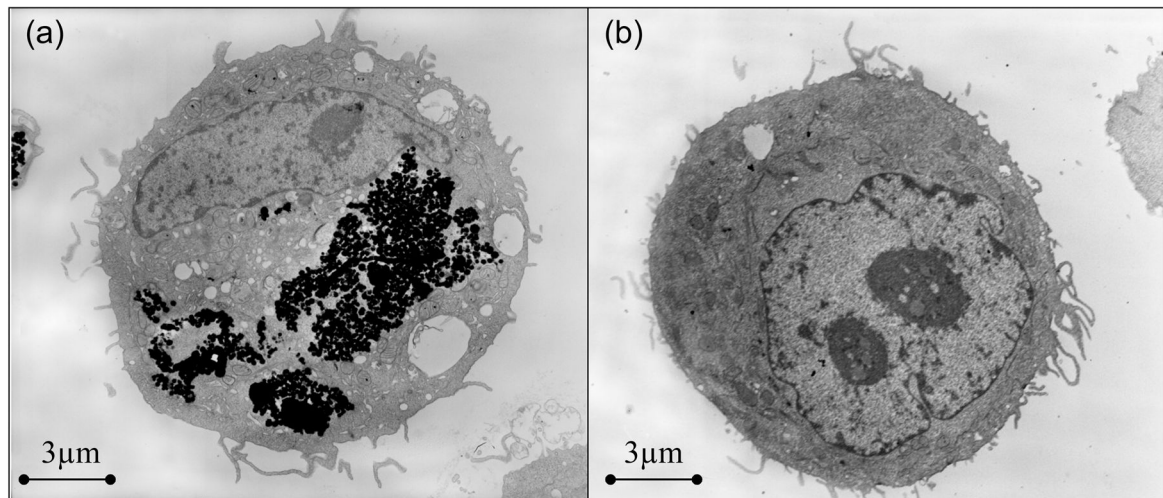
Figure 4.
Transmission electron micrographs of cells cultured with (a) NS-HER (b) NS-HER with pre- and co-treatment of 200 μg/ml free herceptin, for 4h.
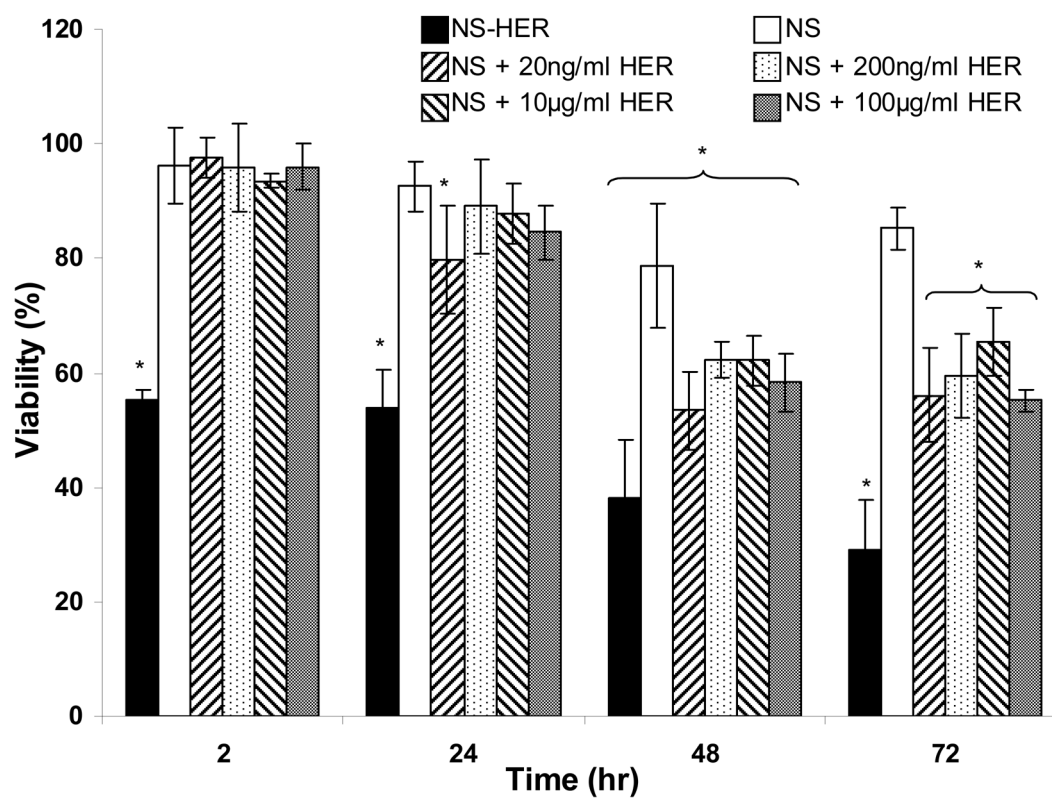
Figure 5.
Cytotoxicities of NS-HER and NS with various concentrations of herceptin, as measured by the viabilities of SK-Br-3 cells grown in media containing 0.2 mg/ml of these nanospheres relative to the non-toxic control. Results are represented as mean ± standard deviation. "*" denotes statistical differences ($P < 0.05$) compared to the control experiment.
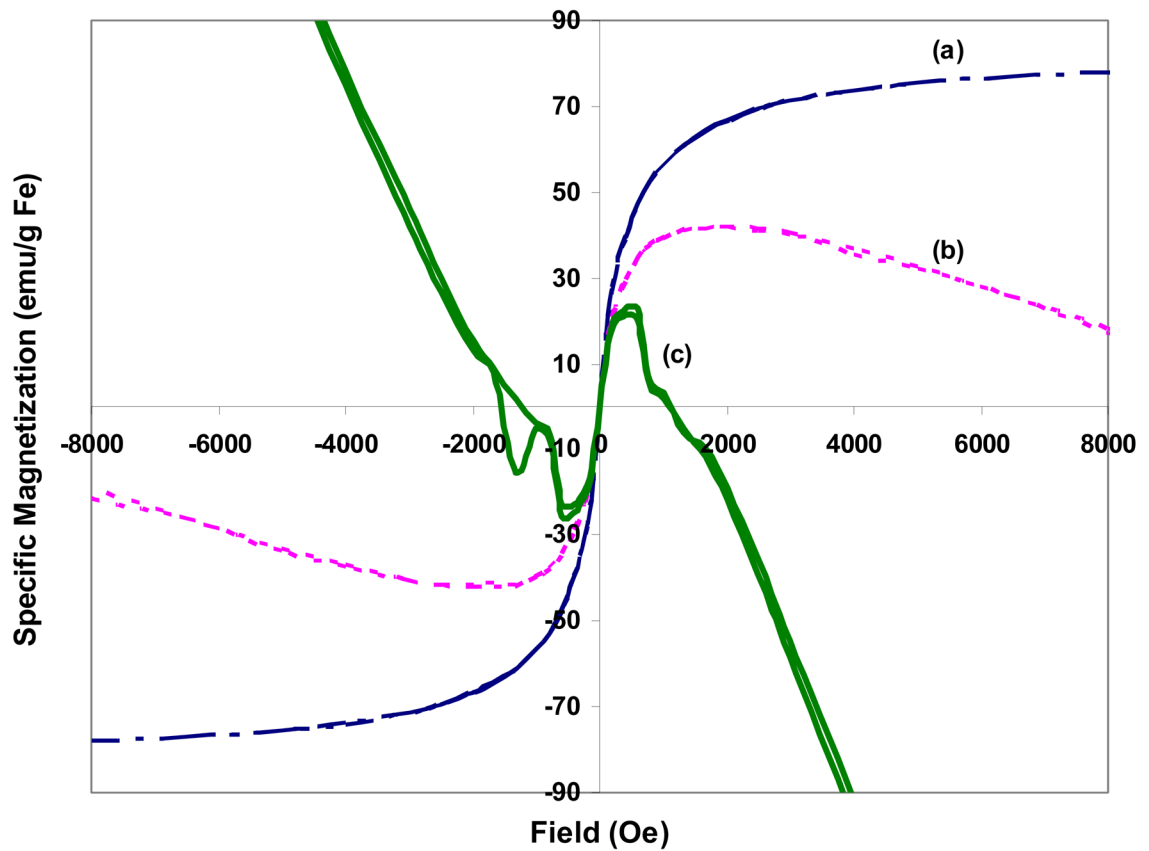
Figure 6.
Magnetization curves of NS-HER in different environments (a) NS-HER solid, (b) NS-HER dispersed in culture medium with 1% agarose and (c) endocytosed NS-HER dispersed in culture medium with 1% agarose.
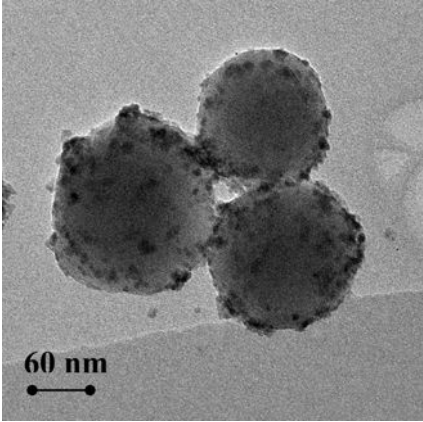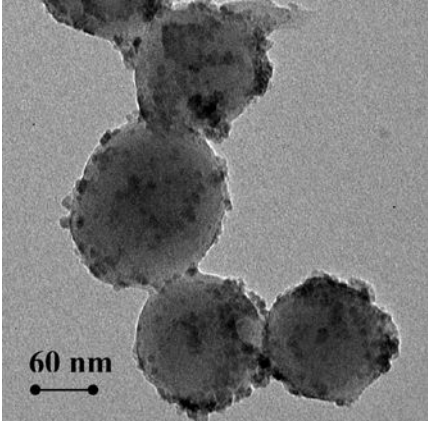
Table 1

Properties of NS, NS-HER

	NS	NS-HER
% Fe	26.8	24.3
D_H (nm)	424 ± 23	752 ± 40
Zeta-Potential (mV)	-9.4 ± 1.6	-4.3 ± 2.0
Morphology (TEM image)		

Table 2

Amount of iron associated with SK-Br-3 and MDA-MB-231 cells after incubation with NS and NS-HER

| Cell line | Iron association (pg/cell) | | | |
	NS		NS-HER	
	2 h	24 h	2 h	24 h
SK-Br-3 (HER-2 Overexpression)	4.6 ± 0.7	9.1 ± 3.1	21.9 ± 4.7	69.6 ± 4.6
MDA-MB-231 (Low HER-2 expression)	7.6 ± 2.8	5.9 ± 0.7	7.4 ± 1.9	10.2 ± 3.8